Discharge Assessment of Compound Channels from Shear Force Analysis using Numerical methods and Genetic Programing

Nibedita Adhikari[1] and Alok Adhikari[2]

1

[1] Deputy Director, Examination, Biju Pattnaik University of Technology, Rourkela, India, drnibeditaadhikari@gmail.com
[2]Research Scholar, Department of Civil Engineering, NIT Rourkela, India, write2aa04@gmail.com

Abstract. Laboratory experimental series were conducted constructing a compound channel to assess the shear stress at the juncture of main channel and floodplain surfaces for varied roughness which influences the discharge of a stream flow. Specifically, evaluation was carried for compound channel floodplains which vary its roughness with season and time. Numerical methods were developed to calculate the shear force (SF). Genetic Programming (GP) was used to evaluate the % SF at different boundary surfaces. Past studies were compared with suggested models and the results gave minimum error than previous findings.

Keywords: Apparent Shear Force, Boundary Shear, Genetic Programming Shear Force,

1 Introduction

Reliable discharge estimation for a river with a main deep channel along with one or more floodplains

is often a difficult task. Quantity of flow accounts for designing of structures, their operation, maintenance and their periphery. Compound channel flow characteristics are complex which is dependent on the velocity field, cross section and boundary roughness. In broader sense other influencing parameters are bed slope, shear, depth ratio, width ratio, sinuosity, viscosity, gravitational forces and most importantly the momentum transfer mechanism (Mohanty et.al 2014).

Main channel flowing on to floodplain/s results slow moving lower depth flow of floodplain retards the flow of main channel and changes when the depth of floodplain increases. There occurs a drag and pull momentum transfer mechanism making carrying capacity of flows more complex. Many researchers have tried to study compound channel flow for different sections. Flow keeping aside of its stage encounters shear along boundaries and shear encountered between adjacent flow layers (Rajaratnam and Ahamadi 1979). Prominent flow interaction takes place at the interface of main channel and floodplain and the momentum transfer takes the form of apparent shear stress (Myers 1978).

Knight and Hamed (1984) experimented boundary shear force distribution for a compound channel, by making floodplain roughened by strip roughness and proposed equation for the percentage of total shear force carried by the floodplain (*% SF_{fp}*) as,

$$\%\mathrm{SF_{fp}} = 48(\alpha - 0.8)^{0.289} 2\beta^{1/\mathrm{m}}\left(1 + 1.02\sqrt{\beta}\log\gamma\right) \quad (1)$$

Where, $\mathrm{m} = \frac{1}{0.75e^{0.38\alpha}}$

in which α is the width ratio of the compound channel (=B/b); *B* is width of compound channel, *b* is the width of main channel base. β is the relative depth (= (H-h)/H), *H* is the depth of compound channel flow in the main channel, *h* is the depth of main channel, Υ is the differential roughness (the ratio of Manning's resistance coefficient of the floodplain boundary (n_{fp}) to that of the main channel boundary (n_{mc}). This equation was developed for low width ratio of α = 4 and γ in the range of 1-3.

Further the Eq.1 was modified by Khatua and Patra (2007) with differential roughness for width ratio of the range 2 to 4,

$$\%\mathrm{SF_{fp}} = 1.23\beta^{0.1833}(38\ln\alpha + 3.6262)\left(1 + 1.02\sqrt{\beta}\log\gamma\right) \quad (2)$$

Khatua et al. (2012) derived an equation for $\%\mathrm{SF_{fp}}$ as a function of floodplain area having width ratio of 6.67 with uniform roughness .They further expressed the percentage of shear force in floodplain as,

$$\%\mathrm{SF_{fp}} = 4.105\left[\frac{100\beta(\alpha-1)}{1+\beta(\alpha-1)}\right]^{0.6917} \quad (3)$$

It was observed that Khatua et al. predicted well (Eq. 3) for the smooth channel, where as gives large errors for channels having differential roughness of main channel and floodplain. Therefore, there was a need for an improvement in the model to successfully predict $\% SF_{fp}$ for such channels.

2 Experimental Arrangements

Experiments are conducted in a straight compound channel having symmetrical flood plains measuring 12m×2m×0.6m in the Hydraulics Engineering laboratory of the National Institute of Technology Rourkela, India. Fabrication of channel was made with Perspex sheet of 0.006 meter thick having uniform Manning`s n value as 0.01. A trapezoidal channel was glued with chemicals and installed inside a tilting flume. The channel has the width ratio (α) as 15.75 and the aspect ratio (δ) of 1.5. Water was supplied to the channel from an underground sump with a re-circulating system through one overhead tank (Fig.1). The experimental channel section is shown in Fig.2. Objective of this work was to know the effect of roughness in the floodplains on the flow behavior during high floods. Therefore observations were carried out in one run with same Perspex sheet roughness in the floodplain (Smooth) and roughened floodplains to other types for different runs. In the floodplains different roughening materials were used to provide the effect of vegetation. For roughening, a synthetic mat was used in the floodplain surfaces having spikes 12mm long 1.5mm width with 72 spikes per square inch (Rough I). Next wire mesh was used for roughening the floodplains (Rough II). In the third case, wire mesh in main channel with crushed stone at floodplains (Rough III) were used while in the fourth case smooth main channel with crushed stone in floodplains were used (Rough IV). Wire mesh used is having mesh opening size of 3mm x 3mm with wire diameter of 0.4mm. Crushed stones used for roughening having equivalent sand roughness of 3.39 mm.

3 Boundary Shear Stress Modelling

Using the Preston tube technique, differential velocities are measured along the wetted perimeter which

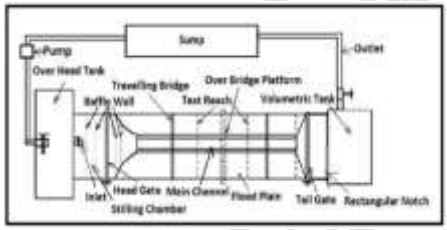

Fig.1. Schematic drawing of experimental system

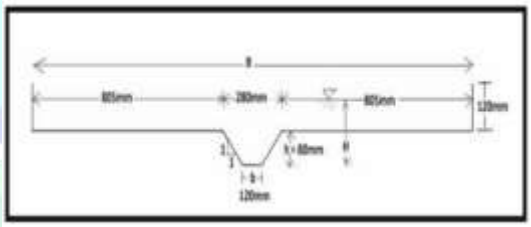

Fig.2. Straight Compound Channel Section

were converted to the boundary shear stress using Patel`s Equation (Khatua et. al 2007). Boundary shear measurements are carried out at the entire cross section for different relative depths of flows, (β) = 0.13, 0.2, 0.3 and 0.34. The shear stress profiles along the rigid surface of the channel are shown in Figure 3 to all the seven sides of the channel; namely the floodplain walls (F-1), floodplain bed (F-2), main channel wall (F-3) and the main channel bed (F-4) and it`s mirroring.

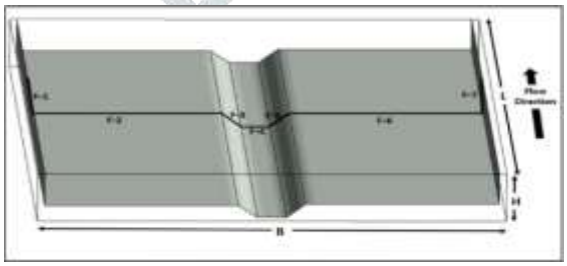

Fig.3. Geometry showing the notations of each boundary for boundary shears distribution

Many investigators found that the boundary shear stress distribution is not uniform over the wetted perimeter (Knight and Demetriou (1983), Knight and Hamed (1984), Khatua and Patra (2007), Knight et al. (2010), Khatua et al. (2010, 2012)). Still boundary shear distribution in compound channel having width ratio, $\alpha > 10$ along with roughness variation is rare to come across.

4 Distribution of Boundary Shear Force

The measured experimental boundary shear stress is integrated over the wetted perimeter to get the shear force at the different regions across the cross-section for each depth of flow can be represented as, Shear force in Floodplain sidewall to main channel bed is given as

$$(F\text{-}i) = \int_{F-i} \tau dp \quad \text{, for i= 1, 2, 3 and 4} \tag{4}$$

The total shear force can be represented as,

$$SF_T = 2SF_{F-1} + 2SF_{F-2} + 2SF_{F-3} + SF_{F-4} \tag{5}$$

Theoretically, $SF_T = \rho g A S$ (6)

Here, SF represents shear force, τ is the boundary shear stress distribution, p represents the respective wetted perimeter and SF_T represents the total shear force. The total shear force is calculated by using Eq.5. The total theoretical shear force is calculated for each section by using Eq.6 and is averaged to compare with the actual values. The error found between the values is less than 10% and is distributed proportionately among the bed and walls.

The floodplain sidewall region (i.e.F-1) is observed to increase its share of shear force with the increase of flow depth for both the cases of floodplain roughness. For same relative depth, the floodplain with roughened materials contributes more in shear force. Similar observation is deduced for the main channel sidewall and the bed (i.e. F-3 and F-4 respectively). The shear force carried by the floodplain bed (F-2) decreases with the relative depth to compensate the increase in the other regions. The main channel sidewalls are noticed to share higher shear force than the main channel bed.

Table 1. The % SF per Length at Different Sections for Straight Smooth Compound Channel

Relative Depth	Flow Depth(m)	SF_T(Exp.) (N/m^2)	SF_T(Actual) (N/m^2)	SF_{F-1}as (% per m) of SF_T	SF_{F-2}as (% per m) of SF_T	SF_{F-3}as (% per m) of SF_T	SF_{F-4} as (% per m) of SF
β = 0.13	0.092	1.712	0.996	17.128	16.127	13.033	3.712
β = 0.2	0.100	2.380	1.420	9.993	20.081	15.861	4.065
β = 0.23	0.104	2.605	1.640	12.760	15.191	17.582	4.466
β = 0.27	0.110	1.986	1.920	14.740	17.342	12.553	5.366
β = 0.32	0.117	2.544	2.268	9.016	16.294	18.657	6.033
β = 0.4	0.132	2.000	3.016	12.041	15.455	16.483	6.021

Table 2. The % SF per Length at Different Sections with Rough Floodplain

Relative Depth	Flow Depth(m)	SF_T(Exp.) (N/m^2)	SF_T(Actual) (N/m^2)	SF_{F-1}as (% per m) of SF_T	SF_{F-2}as (% per m) of SF_T	SF_{F-3}as (% per m) of SF_T	SF_{F-4} as (% per m) of SF_T
β = 0.2	0.100	2.201	1.420	14.689	17.485	14.025	3.801
β = 0.23	0.104	2.276	1.640	14.689	17.372	14.039	3.901
β = 0.27	0.110	1.906	1.918	12.544	14.325	17.874	5.257
β = 0.3	0.115	2.438	2.168	12.123	14.274	17.334	6.269
β = 0.33	0.120	2.547	2.418	10.724	14.775	18.706	5.795
β = 0.36	0.125	1.995	2.666	12.742	15.170	16.179	5.910
β =0.38	0.130	2.025	2.916	12.680	16.043	15.431	5.846

Table 1 depicts the shear force distribution and the percentage of sharing of normalized shear force per length of the channel section from the averaged total theoretical shear force for straight smooth compound channel at face F-1 through F-4. Whereas, the Table 2 shows the sharing of shear force distribution throughout the channel sections for straight compound channel having rough floodplain.

The %SF per unit length in the floodplain side wall is observed to be more in the case of rough channels as compared to the similar value of relative depth in smooth channel. At less relative depth, the % SF per unit length for the floodplain in rough channel is bit more than smooth channel, whereas at higher relative depth it becomes more or less constant. At the main channel side slope, the % SF per unit length is more in the case of rough channels. Similar observation is also seen in the case of main channel bed.

5 Development of Boundary Shear Model

To estimate the boundary shear distribution, the SF on each element of the wetted perimeter (SF_i) of floodplain was obtained by multiplying the adjusted shear stress on each point with appropriate wetted perimeter element of floodplain, and then all were integrated and then doubled to give total shear force carried by the floodplains (SF_{fp}). The % SF is then determined. The % SF carried by the floodplains by the experimental analysis conducted at NITR for different channel roughness and their corresponding flow

depths are recorded for analysis. It is observed that $\%SF_{fp}$ gradually increases with the increase in relative depth in all the channel types. $\%SF_{fp}$ is also observed to gradually decrease with the increases in differential roughness, γ. This may be due to the surface roughness, which reduces the velocity of the flow on floodplain resulting in the decrease in shear force. Simultaneously it increases the velocity in the main channel.

Table 4 illustrates the predicted values of $\%SF_{fp}$ by the Eqs. (1), (2) and (3). To improve the results derived by Khatua et.al a multiplication factor for $\%SF_{fp}$ between the observed and estimated value of Eq. (7) due to the variation of differential roughness is found for all the series. An exponential relation is observed and the modified equation for Eq. (9) is expressed as,

$$\%SF_{fp} = 4.105\left[\frac{100\beta(\alpha-1)}{1+\beta(\alpha-1)}\right]^{0.6917}\left(1-3.22\ln\gamma\, e^{-1.441\beta}\right) \quad (7)$$

Eqs. (1), (2), (3) and (7) are used to determine the $\%SF_{fp}$ and the percentage of error for the different experimental data sets of NITR. The developed model is observed to predict acceptably better results for all the channels with respect to the other models.

6 Apparent Shear Stress

The apparent shear forces (ASF) acts on the imaginary interface of the compound section so that the momentum transfer between the floodplains and the main channel which is evaluated by the percentage of floodplain shear. It provides an insight on the magnitude of interaction between the main channel and the floodplains, which in turn proposes the merits for the selection of interfaces for discharge estimation. The conventional method of calculation of discharge in compound sections divides the channel into hydraulically homogeneous regions by plane originating from the junction of the floodplain and main channel, so that the floodplain region can be considered as moving separately from the main channel. The assumed plane may be, (1) vertical interface; (2) horizontal interface or (3) diagonal interface. The different division methods are illustrated in Figure 5.

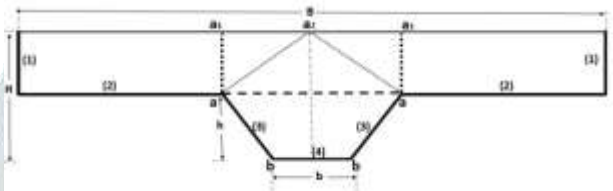

Fig. 5. Division Method in Compound Channel

Because the boundary shear stress carried by the compound section (ρgAS_f) is equal to 100%, where A is the total cross section of the compound channel, the % SF carried by the main channel surfaces can be calculated as;

$$100\frac{\int \tau\, dp\, A_{mc}}{\rho g A S_f} = \%\left[SF_{(3)} + SF_{(4)}\right] = 100\frac{\rho g A_{mc} S_f}{\rho g A S} - 100\frac{ASF_{ip}}{\rho g A S_f} \quad (8)$$

But $\%\left[SF_{(3)} + SF_{(4)}\right] = 100 - \%\left[SF_{(1)} + SF_{(2)}\right]$; and $100\frac{ASF_{ip}}{\rho g A S_f}$ = % SF on the assumed interface. Substituting the values, the ASF on the interface plane can be calculated as

$$\%ASF_{ip} = 100\frac{A_{mc}}{A} - \{100 - \%[SF_1 + SF_2]\} \quad (9)$$

where % ASF_{ip} = percentage of shear force in the interface plane.

For vertical interface between the boundary of the floodplain and main channel shown by the lines aa1 in Fig. 5, the value of A_{mc} is the area marked by a1abbaa1, which when substituted in Eq.(12), yields $\%ASF_V$. Similarly, for horizontal or diagonal interfaces, A_{mc} is estimated from the area marked as aabb or a_2abba_2, respectively, in Fig. 5. This ASF is expressed as percentages of the total channel shear force using the following equations for Vertical (Eq.10), Horizontal (Eq. 11) and Diagonal (Eq. 12) interfaces.

$$\%ASF_V = \frac{50}{[(\alpha-1)\beta+1]} - \frac{1}{2}\{100 - \%[SF_1 + SF_2]\} \quad (10)$$

$$\%ASF_H = \frac{100(1-\beta)}{[(\alpha-1)\beta+1]} - \{100 - \%[SF_1 + SF_2]\} \quad (11)$$

$$\%ASF_D = \frac{25(2-\beta)}{[(\alpha-1)\beta+1]} - \frac{1}{2}\{100 - \%[SF_1 + SF_2]\} \quad (12)$$

% ASF for the three assumed interface planes for the present experimental dataset series of NITR are shown in Table 5 (column 6 & 12) and Table 6 (column 6 & 12). The table compares the measured shear force percentages carried by the floodplains in each

case along with the computed values. It is observed that the average error is minimum for the present experimental model for smooth and all the three cases of floodplain roughness. Again it was concluded that the diagonal division method is a more appropriate method of channel division.

7 Genetic Programming

Genetic programming (GP) is an optimization tool which uses machine learning approach motivated from general biology. It randomly generates a population of computer programs in order to optimize the task. Here the computer programs are internally represented as tree structures. Then mutation and crossover is carried out on best performing trees to find a new population. This process is iterated until the population contains the programs solve the task well. The mathematical models derived in GP are more compact and robust (Azamathulla et.al 2010).

For the current research the open source MATLAB toolbox called GPTIPS is used as it is developed for specific purpose of performing symbolic regression. It employs a unique type of symbolic regression called multigene symbolic regression (Searson 2010) that evolves linear combinations of non linear transformations of the input variables. GP model is composed of nodes, which resembles a tree structure and thus, it is known as GP tree. Nodes are the elements either from a functional set or terminal set. A functional set may include arithmetic operators (+,-,*, /), mathematical functions (sin(.), cos(.), tanh or ln(.)), Boolean operators (AND, OR, NOT, etc), logical expressions (IF, or THEN) or any other suitable functions defined by the users, whereas the terminal set include variables (like *x1, x2, x3*, etc) or constants (like 1,2,3,4 etc.) or both. The functions and terminals are randomly chosen to form a GP tree with a root node and the branches extending from each function node to end in terminal nodes as shown in Fig. 6 for the expression, $y = aX_1 + log\ bX_2$.

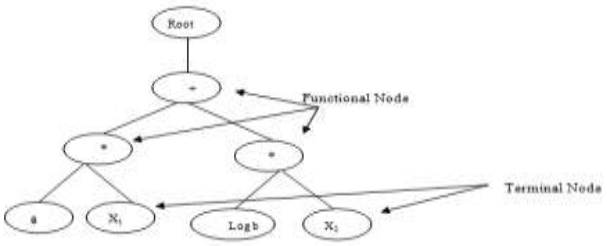

Fig.6. GP Tree for expression $ax_1 + Log\ b\ x_2$

8 Shear Force Prediction using GPTIPS

From previous studies it is observed that different hydraulic parameters play crucial role for fluctuation of discharge data. Using artificial neural networks with stage as single input to predict discharge as the output, different network models are derived earlier. It is observed the model equations derived were much complex. Therefore different common hydraulic characteristics are taken as input for calculation of *SF* for predicting discharge using GP.

9 GPTIPS Run Settings

A GPTIPS run with the following settings is performed for all five models discussed above. Initially a set of GP trees, as per the data sets of each model are randomly generated using various functions and terminals assigned. The fitness criteria calculate the objective function, which determines the best population. At each generation a new population is created through reproduction, crossover and mutation of the selected GP trees in the mating pool. The new population then replaces the existing population. This process is iterated until the termination criterion, which can be either a threshold fitness value or maximum number of generations is satisfied. The best GP model (Table 3), based on its fitness value is selected in order to minimise the root mean squared prediction error on the testing data.

Table 3. Description of GP models for different Data Sets

Model	Training data(Initial population)	Testing data	No. of Generations	Tournament size	D_{max}	G_{max}	Function Node set
Smooth	120	20	77	4	3	5	+,-,*, plog, square
Rough	28	10	0	4	4	5	

Besides the data collected from the present experimental set up data sets from Flood facility at HR Wallingford UK and the reported data from other investigators were taken for analysis (Knight and Demetriou 1983, Myers 1987, Atabay and Knight 2002, and Rezaei 2006). The GP model derived the Eq. 13 after several runs with minimum bias and maximum number of parameters.

$$\%SF_{fp} = 3.445\,\alpha + 12.5\text{plog}(\text{plog}(\alpha(S_0+\beta)) - 3.445\gamma^2\beta^2 + 14.19\alpha(S_0-\beta) + 70.2\text{plog}(\alpha(2S_0+\beta)) + 42.68 \quad (13)$$

where α is width ratio, S_0 the bed slope, γ the differential roughness between floodplain to main channel and β the depth ratio. Percentages of ASF for the three assumed interface planes for the present experimental dataset series of NITR for GP model are shown in Table 4 (column 7 & 13) and Table 5 (column 7 & 13) using Eq. 13. It was observed that GP model even better performed than the suggested experimental model with least average error.

Table 4. Calculation Sheet for $\%S_{fp}$, $\%ASF_V$ and Average Error

Channel Type	$\%SF_{fp}$						$\%ASF_V$					
	Observed	by Knight and Hamed (1984)	by Khatua and Patra (2007)	by Khatua et al. (2012)	By Experimental New Model	by GP model	Observed	by Knight and Hamed (1984)	by Khatua and Patra (2007)	by Khatua et al. (2012)	by Experimental New Model	by GP model
1	2	3	4	5	6	7	8	9	10	11	12	13
Smooth Channel	89.85	104.40	91.15	73.64	73.64	74.35	32.98	40.25	33.63	24.87	24.87	25.23
	90.31	104.56	99.26	81.10	81.10	74.06	28.80	35.93	33.27	24.20	24.20	20.68
	86.59	104.62	102.13	83.21	83.21	73.70	25.32	34.34	33.10	23.64	23.64	18.88
	89.73	104.67	105.06	85.12	85.12	73.12	25.25	32.72	32.92	22.94	22.94	16.95
	85.85	104.72	107.95	86.77	86.77	72.25	21.71	31.15	32.76	22.17	22.17	14.91
	86.49	104.80	112.39	88.92	88.92	69.86	19.65	28.81	32.60	20.87	20.87	11.34
Average Error								**33.87**	**33.05**	**23.11**	**23.11**	**18.00**
Rough Flood-plain	90.19	106.16	100.77	82.34	66.03	74.06	28.74	36.72	34.03	24.81	16.66	20.67
	90.13	106.34	103.81	84.59	68.49	73.69	27.10	35.20	33.94	24.32	16.27	18.88
	85.25	106.54	106.93	86.63	70.88	73.11	23.01	33.65	33.85	23.70	15.83	16.94
	84.78	106.68	109.21	87.98	72.55	71.66	21.59	32.54	33.81	23.19	15.48	15.03
	84.90	106.80	111.14	89.04	73.93	70.74	20.67	31.62	33.79	22.73	15.18	13.59
	86.45	106.91	112.81	89.88	75.09	69.68	20.61	30.84	33.79	22.32	14.93	12.22
	87.50	107.01	114.26	90.58	76.07	68.41	20.42	30.17	33.80	21.96	14.70	10.87
Average Error								**32.96**	**33.86**	**23.29**	**15.58**	**15.46**

Table 5. Calculation Sheet for $\%ASF_H$, $\%ASF_D$ and Average Error

Channel Type	$\%ASF_H$						$\%ASF_D$					
	Observed	by Knight and Hamed (1984)	by Khatua and Patra (2007)	by Khatua et al. (2012)	by Experimental New Model	by GP model	Observed	by Knight and Hamed (1984)	by Khatua and Patra (2007)	by Khatua et al. (2012)	by Experimental New Model	by GP model
1	2	3	4	5	6	7	8	9	10	11	12	13
Smooth Channel	53.20	67.75	54.50	36.99	36.99	37.70	29.79	37.06	30.44	21.68	21.68	22.04
	40.15	54.41	49.10	30.94	30.94	23.91	24.44	31.56	28.91	19.83	19.83	16.31
	31.48	49.51	47.02	28.11	28.11	18.59	20.53	29.55	28.30	18.84	18.84	14.09
	29.58	44.52	44.91	24.97	24.97	12.97	20.02	27.49	27.69	17.71	17.71	11.72
	20.80	39.67	42.90	21.71	21.71	7.20	16.06	25.49	27.11	16.51	16.51	9.26
	14.14	32.45	40.04	16.58	16.58	-2.48	13.36	22.52	26.31	14.58	14.58	5.05
Average Error		**48.05**	**46.41**	**26.55**	**26.55**	**16.31**		**28.95**	**28.13**	**18.19**	**18.19**	**13.08**
Rough Flood-plain	40.03	56.00	50.61	32.18	15.88	23.90	24.38	32.36	29.67	20.45	12.30	16.31
	35.02	51.23	48.71	29.48	13.38	18.58	22.30	30.41	29.14	19.53	11.48	14.08
	25.10	46.39	46.78	26.48	10.73	12.96	17.78	28.42	28.62	18.47	10.60	11.71
	21.00	42.90	45.43	24.20	8.77	7.88	16.05	27.00	28.26	17.65	9.93	9.48

	18.09	40.00	44.34	22.23	7.13	3.94	14.86	25.81	27.98	16.92	9.37	7.78
	17.09	37.55	43.45	20.52	5.72	0.31	14.58	24.81	27.75	16.29	8.89	6.19
	15.94	35.45	42.71	19.02	4.52	-3.15	14.19	23.95	27.58	15.73	8.48	4.65
	Average Error	**44.22**	**46.00**	**24.87**	**9.45**	**9.20**	**Avg. Er-ror**	**27.54**	**28.43**	**17.86**	**10.15**	**10.03**

10. Conclusion

As reported earlier, for computation of discharge of a stream flow with assessment of boundary shear or apparent shear stress, diagonal division method is proved to be the best and using this numerical model is suggested. Again using Genetic Programming, much better prediction is observed in case of smooth and rough floodplains with minimum average error for different cases, which can be used for similar studies with more number of runs of flow or data sets.

References

1. Mohanty, P. K. and Khatua, K.K.: Estimation of Discharge and Its Distribution in Compound Channels, Journal of Hydrodynamics, Vol.26, No.1, pp144-154, (2014).
2. Rajratnam, N. and Ahmadi, R.M.: Interaction between Main Channel and Flood Plain Flows, J. of Hydraul. Eng., ASCE, Vol.105 (HY5), pp.573-588, (1979).
3. Knight, D. W. and Hamed, M. E.: Boundary Shear in Symmetrical Compound Channels, J. of Hydraul. Eng., ASCE, Vol. 110, paper 19217, pp. 1412-1430, (1984).
4. Khatua, K.K. & Patra, K.C.: Boundary shear stress distribution in compound open channel flow. J. Hydr. Eng., ISH, Vol. 12, No.3, pp. 39-55, (2007).
5. Khatua, K.K., Patra, K. C. and Jha, R.: Apparent shear stress in compound channels. J. Hydraul. Res., (ISH), Special issue, Taylor & Francis, vol. 16, no. 3, pp. 1-14, Dec, (2010).
6. Khatua, K. K., Patra, K. C. and Mohanty, P. K.: Stage Discharge Prediction for Straight and Smooth Compound Channels with Wide Floodplains. J. Hydraul. Eng., ASCE, vol. 138(1): 93-99, (2012).
7. Knight, D. W. and Demetriou, J. D.: Floodplain and Main Channel Flow Interaction, J. of Hydraul. Eng., ASCE, 109(8), 1073-1092, (1983).
8. Knight, D. W., Tang, X., Sterling, M., Shiono, K. and McGahey, C.: Solving open channel flow problems with a simple lateral distribution model, River Flow, vol. 1, pp. 41-48, (2010).
9. Azamathulla, H. Md. and Aminuddin, Ab Ghani.: Genetic Programming to Predict River Pipeline Scour, Journal of Pipeline Systems Engineering and Practice, ACSE, Vol.1, No. 3, pp.127-132, (2010).
10. Searson, D. P., David, E. Leahy. and Mark, J. Willis.: GPTIPS: An Open Source Genetic Programming Toolbox for Multigene Symbolic Regression; Proc. Of Int. Conference of Engineering and Computer Scientists, Vol. I, IMECS2010, March17-19, (2010).
11. Knight, D.W. and Demetriou, J.D.: Flood plain and main channel flow interaction, Journal of Hydraulic Engineering, ASCE, 109(8), pp. 1073-1092, (*1983).*
12. Myers, W.R.C.: Velocity and discharge in compound channels, Journal of Hydraulic Engineering, ASCE, Vol.113 (6), pp. 753-766, (1987).
13. Atabay, S.A. and Knight, D.W.: The Influence of Floodplain width on the Stage Discharge Relationship for compound Channels, River Flow, Proceeding of Int. Conference on Fluvial Hydraulics, Louvail- La-NEUVE, Belgium, Vol.1, pp.197-204, (2002).
14. Rezaei, B. (2006). Overbank flow in compound channels with prismatic and non-prismatic floodplains, Diss. University of Birmingham.